JCTC Journal of Chemical Theory and Computation

Article

pubs.acs.org/JCTC

# CHARMM-GUI Martini Maker for Coarse-Grained Simulations with the Martini Force Field

Yifei Qi,[†] Helgi I. Ingólfsson,[‡] Xi Cheng,[†] Jumin Lee,[†] Siewert J. Marrink,[‡] and Wonpil Im*[,†]

[†]Department of Molecular Biosciences and Center for Computational Biology, The University of Kansas, 2030 Becker Drive, Lawrence, Kansas 66047, United States

[‡]Groningen Biomolecular Sciences and Biotechnology Institute and Zernike Institute for Advanced Materials, University of Groningen, Nijenborgh 7, 9747 AG Groningen, The Netherlands

Supporting Information

**ABSTRACT:** Coarse-grained simulations are widely used to study large biological systems. Nonetheless, building such simulation systems becomes nontrivial, especially when membranes with various lipid types are involved. Taking advantage of the frameworks in all-atom CHARMM-GUI modules, we have developed CHARMM-GUI *Martini Maker* for building solution, micelle, bilayer, and vesicle systems as well as systems with randomly distributed lipids using the Martini force field. *Martini Maker* supports 82 lipid types and different flavors of the Martini force field, including polar and nonpolar Martini, Dry Martini, and ElNeDyn (an elastic network model for proteins). The qualities of the systems generated by *Martini Maker* are validated by simulations of various examples involving proteins and lipids. We expect *Martini Maker* to be a useful tool for modeling large, complicated biomolecular systems in a user-friendly way.


## INTRODUCTION

Cell membranes form a highly complex and heterogeneous mixture of membrane proteins and lipids. Despite technical advances, our current understanding of the detailed organization of cellular membranes remains elusive. Characterization of the structural heterogeneity *in vivo* is very challenging, owing to the dearth of experimental methods suitable for studying these fluctuating nanoscale assemblies in living cells with the required spatiotemporal resolution. Computer simulations have become a unique investigatory tool for understanding the supramolecular organization of cellular membrane components, and this "computational microscopy" has become indispensible as a complement to traditional microscopy methods.[1]

State-of-the art molecular dynamics (MD) simulations at the atomic level provide detailed interactions of these membrane components.[2,3] However, in order to simulate the collective behavior of thousands of lipids and proteins for time scales inaccessible for an all-atom level of resolution, coarse-grained (CG) models have gained a lot of popularity lately.[4] Different strategies exist to derive CG models, which can be divided into bottom-up and top-down approaches.[5,6] The former uses more detailed structural data (either from all-atom models or experiments) to systematically derive the CG interactions, whereas the latter relies on direct reproduction of a variety of experimental observables. The Martini force field (FF) combines both bottom-up and top-down approaches and is currently the most widely used CG model.[7] Recently, the Martini FF has been extended to include a large set of biologically relevant lipids, and a variety of tools have been developed for high-throughput membrane protein modeling.[8−13]

In this work, to further enable high-throughput modeling and simulations of cellular membranes of arbitrary shape and complexity, we describe *Martini Maker*, a new tool developed in CHARMM-GUI (http://www.charmm-gui.org).[14] CHARMM-GUI provides a web-based graphical user interface to generate various molecular simulation systems and input files (for CHARMM,[15] NAMD,[16] GROMACS,[17] AMBER,[18] and OpenMM[19] programs) to facilitate and standardize the usage of common and advanced simulation techniques. Within the frameworks of *Quick MD Simulator*,[14] *Membrane Builder*,[20−22] *Micelle Builder*,[23] and *PACE CG Builder*[24] in CHARMM-GUI, *Martini Maker* (http://www.charmm-gui.org/input/martini) facilitates Martini system building for solution, micelle, bilayer, and vesicle simulations as well as simulations starting with randomly distributed detergent/lipid molecules. The supported versions of the Martini FF include standard Martini,[25−27] Martini with polarizable water,[28,29] Dry Martini,[30] and ElNeDyn using elastic networks for proteins.[31] The generated simulation input files are ready for use with the latest GROMACS simulation software.

In the following, we describe the setup of *Martini Maker* and the steps required for users to generate their own systems in detail. To illustrate that *Martini Maker* is robust and well-suited for various types of CG simulations, the results from the following example systems are presented and discussed: three

**Received:** May 31, 2015
**Published:** August 14, 2015





DOI: 10.1021/acs.jctc.5b00513
J. Chem. Theory Comput. 2015, 11, 4486−4494

different bilayer systems, micelle systems starting from preassembled micelles or randomly distributed detergents, and vesicle systems with explicit or implicit CG water.

## METHODS

**Martini Models and Lipid Types Supported.** *Martini Maker* supports a number of different versions of the Martini FF (Table 1). Four protein models are supported, namely,

**Table 1. Martini Models Provided in *Martini Maker***

| model name | protein | water | lipids |
|---|---|---|---|
| Martini22 | Martini 2.2 | Nonpolarizable | Martini 2.0 |
| Martini22P | Martini 2.2 Polar | Polarizable | Martini 2.0 |
| ElNeDyn | 2.2 + Elastic Network | Nonpolarizable | Martini 2.0 |
| ElNeDynP | 2.2P + Elastic Network | Polarizable | Martini 2.0 |
| Dry Martini | | | Dry Martini |

Martini 2.2[26,28] and Martini 2.2 with the ElNeDyn Elastic Network model,[31] both used in combination with either polarizable[29] or nonpolarizable Martini water model. For lipids, in addition to Martini 2.0, an implicit-solvent lipid model named Dry Martini[30] is available in the membrane-only *Bilayer* and *Vesicle Builder*.

In the current implementation of *Martini Maker*, a total of 82 lipid types are supported, covering a large part of the Martini lipidome[12] from sterols to glycolipids (18 of these lipids are available in Dry Martini; see Supporting Information Table S1). The approximate area per lipid of each lipid type, which is used to determine initial system size in *Bilayer* or *Vesicle Builder*, was taken from the areas of all-atom lipids when available or estimated using the Voronoi tessellation method on a 200 ns simulation of a CG membrane that consists of 6711 lipids in total.[32]

**System Building.** The building procedure of membrane systems in *Martini Maker* follows the five general steps in CHARMM-GUI *Membrane* and *Micelle Builder*.[21,23,24]

In STEP 1, in the case of a protein/bilayer, protein/micelle, or protein/vesicle system, the protein structure can be read-in through *PDB* Reader[33] either by uploading a PDB structure file containing single or multiple chains or by typing a PDB ID from the PDB[34]/OPM database;[35] we note that the PDB structure from OPM is preoriented along the *z*-axis, i.e., along the membrane normal, with the bilayer center at $z = 0$. The structure is then converted to CG representation using the secondary structure assignment from DSSP[36] and the martinize.py script.[28] In STEP 2, if necessary, the protein can be aligned to and/or translated along the *z*-axis, and pore water can be generated in the case of a channel protein. In STEP 3, the system size is determined based on the user input, and pseudo atoms are packed to determine the initial positions for lipid headgroups. In *Vesicle Builder*, the protein is translated to the vesicle surface in this step (see below). In STEP 4, the system components including lipids, ions, and water box are generated. In STEP 5, all of the components are assembled to form an initial simulation system, and simulation input files are generated. *Solution Builder* shares STEP 1 with membrane systems, but it generates system components in STEP 2 and assembles them in STEP 3.

The details of each step in *Solution*, *Micelle*, and *Bilayer Builder* are already published.[14,21,23] Here, we focus on unique features in *Vesicle Builder*. Given a specific vesicle radius and lipid composition, building and simulating a vesicle system is not trivial because determining the correct number of lipids in the inner and outer leaflets, as well as the amount of interior solvent, can be very tricky.[37,38] *Vesicle Builder* provides users with a simulation system in which the lipid numbers in the inner and outer layers as well as interior water can be equilibrated within a relatively short simulation time. To allow lipid flip-flop between the leaflets, six water pores are created along the *x*, *y*, and *z* axes by applying cylindrical repelling forces to the lipid tails (Figure 1); N.B., the interior and exterior water molecules are freely exchanged through these water pores.[37,38] The water-filled pores with a radius of 20 Å are initially formed in STEP 3 when pseudo lipid atoms are packed on the inner (radius = $R - 20$ Å) and outer (radius = $R + 20$ Å) leaflets of the vesicle, where $R$ is a user-specific vesicle radius. In STEP 4, lipid structures from a structure library are randomly selected and rotated/translated to bring the headgroup to the pseudo atom position. During equilibration simulations, the water pores are gradually closed when the ratio of lipids of the inner and outer layers reaches equilibrium.

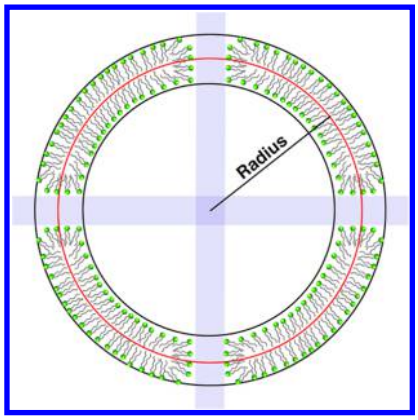


**Figure 1.** Two-dimensional schematic of the vesicle structure from *Vesicle Builder*. Six water pores are created along *x*, *y*, and *z* axes to facilitate lipid flip-flop between the inner and outer layers during equilibration simulations. The vesicle radius is defined as the distance from the center of the vesicle to the center of the bilayer.

**Simulation Protocol.** *Martini Maker* provides (equilibration and production) simulation inputs compatible with GROMACS 4.5[17] or newer. For vesicle simulations, GROMACS 5.1 or newer is required to apply the cylindrical restraints to the lipid tails to maintain the vesicle water pores (Figure 1). In explicit-solvent systems from *Solution*, *Bilayer*, *Micelle*, *Vesicle*, and *Random Builder*, the Lennard-Jones interactions are smoothly switched off at 9−12 Å and the Coulombic interactions are shifted off at 0−12 Å. The time step is 20 fs. The relative dielectric constant is 15 or 2.5 for systems with nonpolarizable or polarizable water, respectively. Pressure is set to 1 bar using the Berendsen barostat[39] with a coupling constant of 5 ps and a compressibility value of $3 \times 10^{-5}$ $bar^{-1}$ for bilayer systems and $4.5 \times 10^{-5}$ $bar^{-1}$ for other systems. Temperature is maintained at 303.15 or 310 K with the velocity rescaling method.[40] In implicit-solvent systems using the Dry Martini model, the leapfrog stochastic dynamics integrator[41] is used to maintain the temperature at 303.15 K with an inverse friction constant of 4 ps. The time step of Dry Martini simulations is 40 fs, and the nonbonded interactions are calculated in the same way as in explicit-solvent systems. During the equilibration of dry bilayer systems, the Berendsen barostat is used to relax the pressure. The semi-isotropic pressure coupling is used by setting the reference pressure to 0


DOI: 10.1021/acs.jctc.5b00513
J. Chem. Theory Comput. 2015, 11, 4486−4494

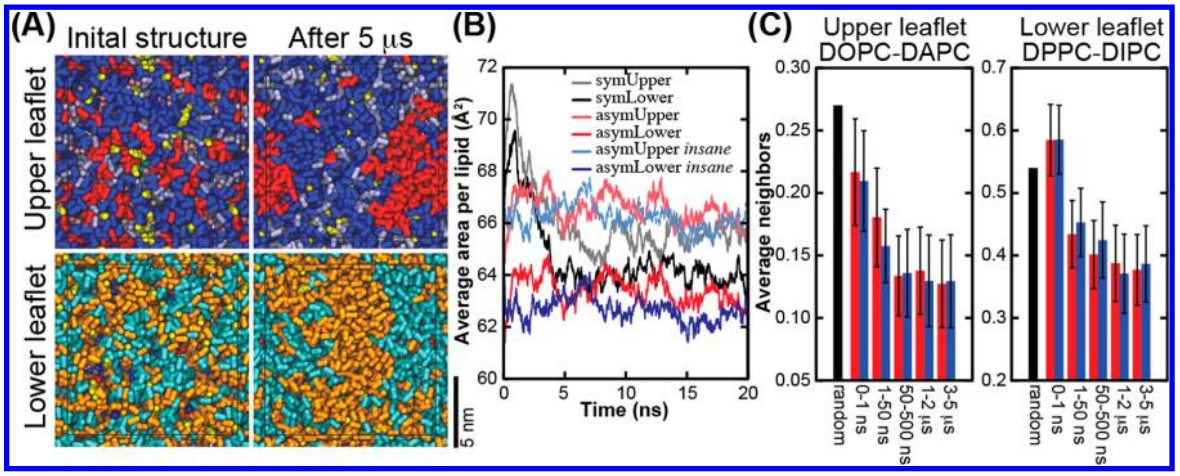


**Figure 2.** Lipid mixing. (A) Snapshots of the upper (DOPC, blue; DAPC, red; DLPC, ice blue; and cholesterol, yellow) and lower (DPPC, orange; DIPC, cyan; and cholesterol, yellow) leaflets after initial setup with *Bilayer Builder* and 5 $\mu$s simulation. (B) Average area per lipid for the upper and lower bilayer mixtures from two simulations with a symmetric composition of each mixture (black and gray) and asymmetrical simulations setup with *Bilayer Builder* (red and light red) and *insane* (blue and light blue). (C) Average number of neighbors (defined as having $PO_4$ beads within an 8 Å cutoff) for the main phase separating lipid in the upper (DOPC-DAPC) and lower (DPPC-DIPC) leaflets. A random mixture (black), assuming all lipids are of the same size, is compared with different time averaging from simulations setup with *Bilayer Builder* (red) and *insane* (blue).

bar, time constant to 4.0 ps, and compressibility to $3 \times 10^{-4}$ and 0 $bar^{-1}$ on the bilayer plane and normal, respectively. The *NVT* ensemble is used for the production step of dry bilayer systems and all steps of dry vesicle systems.

**Trajectory Analysis.** Trajectory analysis was preformed with GROMACS[17] and VMD.[42] In vesicle systems, the vesicle radius is calculated as the middle of the two peaks on the histogram of lipid head groups along the radial distance from the vesicle center. The lipids are assigned to the inner or outer layer by comparing the radial distance of each lipid headgroup to the vesicle radius.

## RESULTS AND DISCUSSION

*Martini Maker* provides five different modules: *Solution Builder*, *Bilayer Builder*, *Micelle Builder*, *Vesicle Builder*, and *Random Builder*. Since building and simulating a solution system (i.e., protein/water systems without any lipids) are relatively trivial, we will skip *Solution Builder* and focus on results from membrane systems in this work.

***Bilayer Builder*: Asymmetric Raft-Forming Membranes.** To demonstrate the building of bilayers using *Bilayer Builder*, an asymmetric raft-forming membrane was built and simulated. The upper leaflet contains a 6:2:2:1 mixture of DOPC, DAPC, DLPC, and cholesterol, and the lower leaflet, a 6:4:1 mixture of DPPC, DIPC, and cholesterol (Figure 2A; see each lipid's nomenclature in Table S2). Note that for a large complex asymmetrical bilayer, the area per lipid for each leaflet needs to be determined from separate independent symmetrical simulations of each bilayer leaflet lipid composition, as the area depends on the exact mixture and environmental factors such as ion concentration and temperature. Therefore, the average area per lipid was measured in symmetrical simulations of each (upper or lower leaflet) composition, giving an average area per lipid of 66.3 $Å^2$ for the upper and 63.1 $Å^2$ for the lower leaflet (averaged over the last 4 $\mu$s of the 5 $\mu$s simulations). Additionally, cholesterol will flip-flop between the leaflets, and if it preferentially aggregates in one leaflet over the other, then the average area should be adjusted accordingly, but this was not done in this illustrative case. After adjusting the final lipid number in each leaflet based on different average area per lipid in the two leaflets (from the symmetrical simulations), the asymmetrical membrane was setup with 220 lipids in the upper and 231 lipids in the lower leaflet. The membrane was then fully hydrated in 150 mM NaCl solution. An identical bilayer was setup using *insane*[12] (a script-based bilayer building program), and both were simulated for 5 $\mu$s. Both of the asymmetrical membrane simulations equilibrate their area per lipid rather fast to values similar to those from the two symmetrical simulations (Figure 2B). The initial bilayer structure from *insane* is less compact than that from *Bilayer Builder* but relaxes fast (<0.5 ns) to within the regular fluctuations of the box area (Figure S1). Note that the calculated average area per lipid (box area/lipid count) fluctuates wildly due to pressure coupling and bilayer undulations. The phase separation of the lipids in the upper and lower leaflets takes much longer to equilibrate (Figure 2C) but is also similar for both simulations (setup with *Bilayer Builder* or *insane*).

***Bilayer Builder*: Complex Plasma Membrane Mixtures.** To demonstrate the feasibility of creating a large bilayer with complex lipid mixture using *Bilayer Builder*, we reconstructed the plasma membrane mixture based on a previous work.[32] The lipid mixture consists of 63 different lipid types asymmetrically distributed across the two leaflets (Figure 3A), which mimics the composition of an idealized mammalian plasma membrane. The simulated membrane contains 6664 lipids fully hydrated in 150 mM NaCl solution. Weak position restraints were added to the *z*-positions of the POPC and PIPC headgroups in the outer leaflet to dampen large-scale bilayer undulations (see each lipid's nomenclature in Table S2). After standard *Bilayer Builder* minimization and equilibration steps, the membrane was simulated for 5 $\mu$s (Figure 3B) and resulted in similar dynamics as that observed in the previous work.[32] In short, cholesterols, ceramides, and diacylglycerols flip-flop between the leaflets on the simulation time scale, and the cholesterol enrichment in the outer leaflet is maintained due to cholesterol's preferred interactions with the outer leaflet lipid composition. Neither leaflet phase-separates, but the lipids are heterogeneously mixed at different time and length scales. Saturated lipid tails prefer other saturated tails and cholesterol, whereas polyunsaturated


DOI: 10.1021/acs.jctc.5b00513
J. Chem. Theory Comput. 2015, 11, 4486−4494

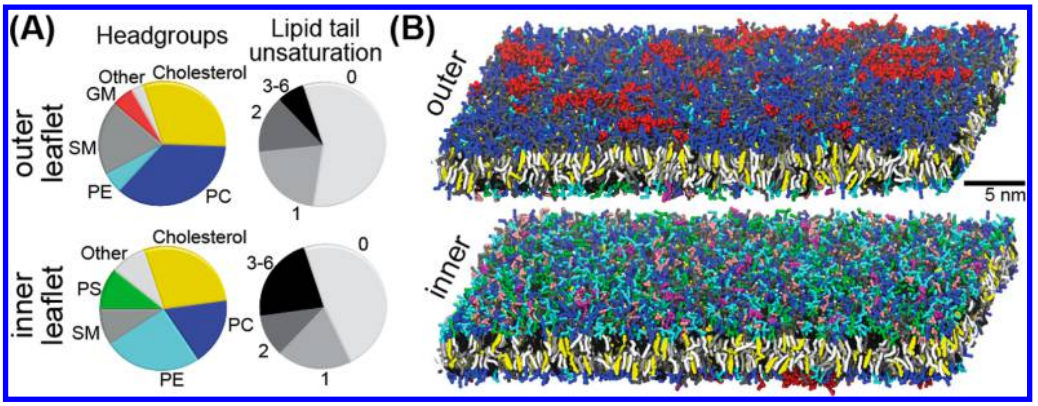


**Figure 3.** An idealized plasma membrane constructed using *Bilayer Builder* following the same composition as that in a previous work.[32] The membrane contains 63 different types of lipids asymmetrically distributed between the outer and inner leaflets. (A) The headgroup composition for the main lipid species and level of tail saturation for the two leaflets. (B) Snapshots of the outer and inner leaflets after 5 $\mu$s simulation. The lipids are colored according to (A).

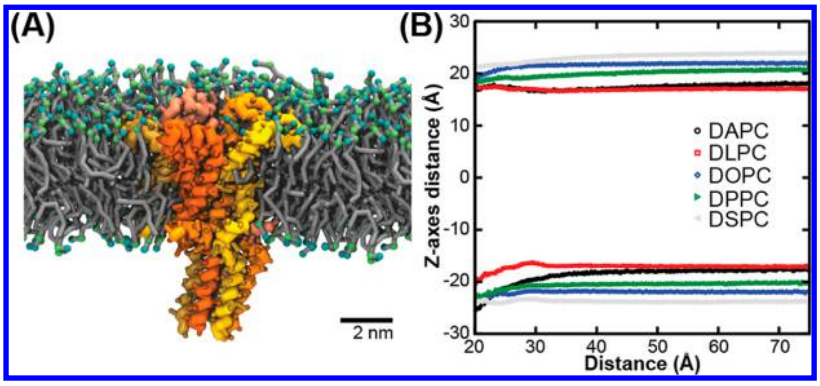


**Figure 4.** MscL embedded in different bilayers. (A) A snapshot of MscL embedded in a DOPC bilayer, fully hydrated in 150 mM NaCl solution, and simulated for 5 $\mu$s. The five monomers of MscL are colored separately, and DOPC is depicted as a gray stick with blue and green balls for the phosphate ($PO_4$) and choline (NC3) headgroups, respectively. (B) The radial position of the bilayer plane (lipid $PO_4$ beads) as a function of radial distance from the MscL channel transmembrane pentamer center. The bilayer is centered at $z = 0$. Note that very few lipids get closer then 20 Å to the channel center and there is a reduced lipid density until ~25 Å.

tails prefer other polyunsaturated tails and dislike cholesterol. The larger patches of increase/decreased cholesterol density are somewhat correlated between the two leaflets, whereas smaller scale patches are not. In the outer leaflet, ganglioside lipids (GM) form clusters/nanodomains (Figure 3B, top colored in red), and in the inner leaflet, pohosphatidylinositol mono, bis, and tris phosphates (PIPs) form dimers and trimers much more frequently than expected at their concentration (Figure 3B, bottom colored in purple).

***Bilayer Builder*: Membrane Proteins Embedded in Bilayers.** In Martini Maker, proteins are embedded in bilayers with the general five-step CHARMM-GUI *Membrane Builder* method; see the Methods section and Jo et al.[22] To illustrate CG Martini membrane protein simulations in bilayers, the mechanosensitive channel of large conductance (MscL) was embedded in five different bilayers using *Bilayer Builder* (Figure 4A). MscL opens to a large mostly unselective pore (~3 nS) with induced membrane tension[43] and serves as a last resort release valve to protect bacteria from lysis upon acute osmotic downshock. Using Martini, MscL gating with induced membrane tension was successfully simulated before.[44] Here, we embedded MscL in its closed state (derived from PDB 2OAR[45] and setup using the Martini22 model in Table 1) in DAPC, DLPC, DOPC, DPPC, and DSPC bilayers and monitored the bilayer profile around the channel for the different lipid types (see each lipid's nomenclature in Table S2). Due to the protein-bilayer hydrophobic adaptation, there is a small compression of the thicker DSPC bilayer and a small expansion of the thinner DLPC bilayer around the channel, whereas the more plastic polyunsaturated DAPC shows the largest adaptation (Figure 4B).

***Micelle Builder* and *Random Builder*.** *Micelle Builder* provides simulation systems starting from preassembled micelles. As a test case, a preassembled micelle with 62 sodium dodecyl sulfate (SDS) molecules was simulated for 1 $\mu$s (Figure 5A,B). The micelle structure is stable during the simulation, and the radius of gyration is 15.8 ± 0.2 Å (Figure 5C), comparable to values from previous coarse-grained (15.7 ± 0.2 Å[46] and 15.5 ± 0.1 Å[47]) and all-atom simulations (15.1 ± 0.1 Å[23]).

When the detergent/lipid assembly process is of interest, it is necessary to start with randomly distributed detergents/lipids.[48−50] To this end, we developed *Random Builder*, which randomly places a certain number of detergents/lipids (with or without proteins) in a given cubic box. In the first test system, we simulated 62 randomly placed SDS detergent molecules for 1 $\mu$s (Figure 5D,E). The SDS molecules assembled into a micelle within 50 ns. The radius of gyration of the assembled micelle is 15.8 ± 0.2 Å in the last 0.5 $\mu$s, in agreement with the result from the preassembled SDS micelle simulation using *Micelle Builder* (Figure 5F). In a second test system, 55 SDS


DOI: 10.1021/acs.jctc.5b00513
J. Chem. Theory Comput. 2015, 11, 4486−4494

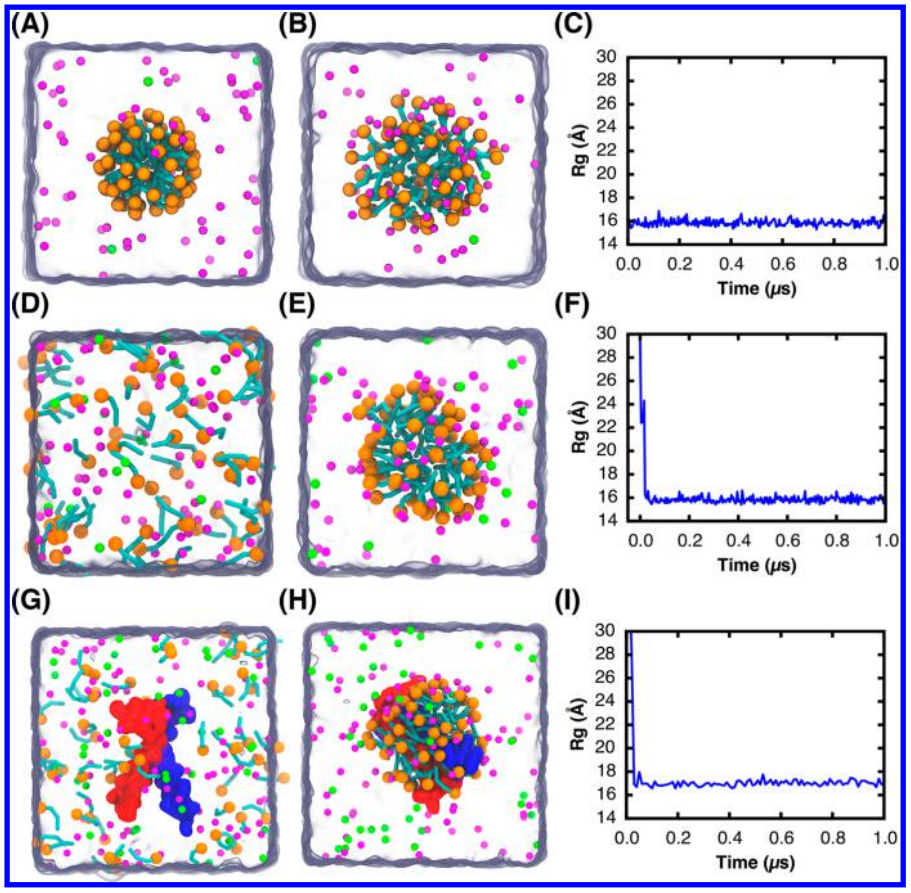


**Figure 5.** Test systems in *Micelle Builder* and *Random Builder*. (A–C) A preassembled SDS micelle using *Micelle Builder*. (D–I) Randomly placed SDS molecules without (D–F) and with (G–I) protein. The first column shows the initial structure, the second column the last snapshot, and the third column the radius of gyration of the SDS molecules. SDS molecules are shown in cyan sticks with an orange headgroup, sodium ions in magenta spheres, and chloride ions in green spheres. Glycophorin A dimer is shown in red and blue surface.

molecules are randomly placed around a glycophorin A (GpA) transmembrane dimer[51] using the Martini22 model (Figure 5G–H). The radius of gyration of the SDS molecules reaches 17.1 ± 0.3 Å in the last 0.5 μs (Figure 5I), comparable to the value from a previous all-atom simulation.[52] About 45 SDS molecules are in direct contact with the protein (Figure S2), whereas the remaining molecules reside on the micelle surface.

***Vesicle Builder*: Estimation of the Initial Number of Lipids in Inner and Outer Layers at a Given Vesicle Radius.** In *Vesicle Builder*, a user can specify the vesicle radius ($R$), the lipid types, and the ratio of different lipids (*Ratio*) in the whole vesicle. However, given these inputs, there is no prior rule to determine the optimal number of lipids in the inner and outer leaflets. To estimate the relationship among the vesicle radius, the total number of lipids ($N_{\text{lipid}}$), and the lipid ratio in the inner and outer leaflets, different sizes of vesicles (2000, 3000, 4000, and 5000 for DPPC and 2000 and 3000 lipids for 16 different lipid types listed in Table S3) were simulated for 240 ns (Figure 6). The four data points from DPPC vesicles were used to fit two functions

$$N_{\text{lipid}} = aR^2 + bR + c \quad (1)$$

$$Ratio = R^n/(R^n + p^n) \quad (2)$$

where $a$, $b$, $c$, $n$, and $p$ are adjustable parameters (Figure S3). For the other 16 lipid types, only two data points are available. These two data points were fitted to the functions by fixing $a$, $b$, and $n$ to the values from DPPC and varying $c$ and $p$ (Table S3). Due to limited computational resources, simulations were not carried out for the other 65 lipid types in Table S1. Parameters $c$ and $p$ were determined by assuming a linear relationship between the area per lipid and these two parameters (Figure S4). Note that these fittings are by no means physical, but they are used during the vesicle building to provide an initial vesicle structure with a reasonable number of lipids in its inner and outer leaflets.

***Vesicle Builder*: Mixed Lipid Vesicles.** To simulate mixed-lipid vesicles, it is important that the relative populations of the lipids in the inner and outer leaflets are allowed to properly equilibrate. In order to achieve this, we have implemented an automated protocol that creates water pores in the vesicle with the cylindrical potentials (see Figure 1). To illustrate the distribution of different lipid types in a vesicle, two mixed DPPC/DPPE and POPC/POPE vesicle systems (with an initial radius of 90 Å) starting with PC/PE = 1:2, 1:1, and 2:1 in both layers were simulated for 550 ns (Figure 7). In these simulations, the water pores remain open with a radius of 20 Å for 500 ns to allow full PC/PE exchange between both leaflets and are closed gradually in the last 50 ns. In both systems, PE is enriched in the inner leaflet because PE has a smaller headgroup and thus fits better to the concave surface in the inner layer than the PC headgroup. Similar results are observed in previous mixed lipid vesicle simulations.[38] The final radii of the vesicles are around 84 Å, which is only 6 Å smaller


DOI: 10.1021/acs.jctc.5b00513
J. Chem. Theory Comput. 2015, 11, 4486–4494

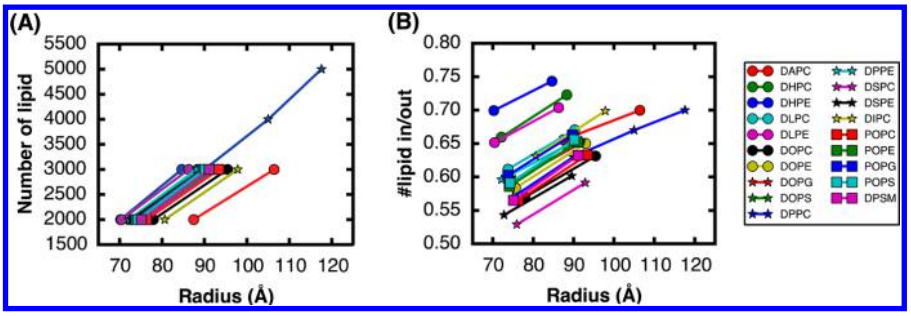


**Figure 6.** (A) Total number of lipids as a function of vesicle radius. (B) The ratio of lipids in the inner and outer layers as a function of vesicle radius.

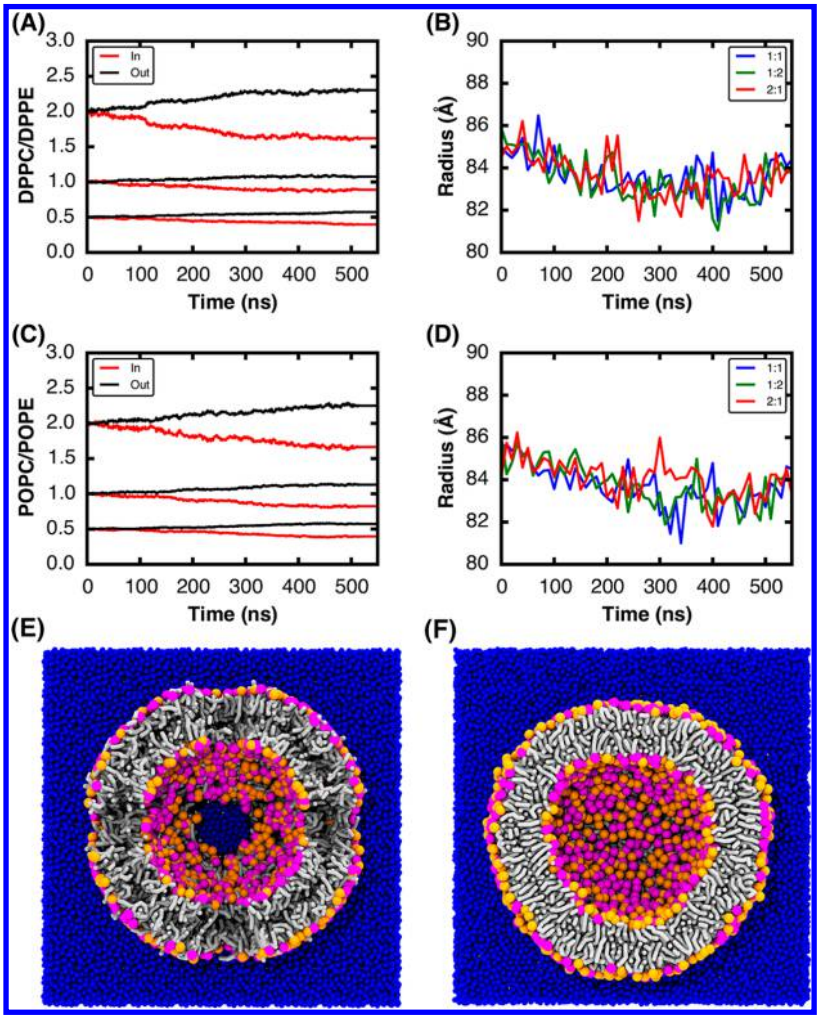


**Figure 7.** Mixed-lipid vesicle systems. (A–D) The ratios of PC/PE in the inner and outer layers and the vesicle radii for (A, B) DPPC/DPPE and (C, D) POPC/POPE starting with 1:2, 1:1, and 2:1 PC/PE ratios. (E, F) The initial and final structures of DPPC/DPPE starting with a 1:1 ratio. POPE headgroups are shown in magenta spheres, DPPC headgroups in orange spheres, lipid tails in stick, and water molecules in blue spheres.

than the target radius of 90 Å. A possible cause of the radius difference is the error in the fitting method.

***Vesicle Builder*: Dry Martini POPC Vesicle.** Dry Martini provides an implicit-solvent lipid model that is especially useful in studying large membrane systems. Although Dry Martini is available in the membrane-only *Bilayer* and *Vesicle Builder* in *Martini Maker*, we illustrate Dry Martini in *Vesicle Builder* by setting up a dry POPC vesicle with an initial radius of 80 Å, which results in 800 and 1372 POPC molecules in the inner and outer layers in the starting structure. The system was simulated for 430 ns of equilibration with all water pores open, 80 ns of equilibration for pore closing, and 100 ns of production. During equilibration, about 45 POPC molecules move from the inner layer to the outer layer (Figure 8A). The vesicle radius drops to ~77 Å in the initial steps of equilibration and reaches 75.4 ± 0.6 Å after the pores are closed (Figure 8B).

## CONCLUSIONS

A typical *Martini Maker* job takes several minutes to a few hours, depending on the system size and server load. A benchmark is listed in Table S4 to show the time required to build several lipid-only bilayer, vesicle, and randomly


DOI: 10.1021/acs.jctc.5b00513
J. Chem. Theory Comput. 2015, 11, 4486–4494

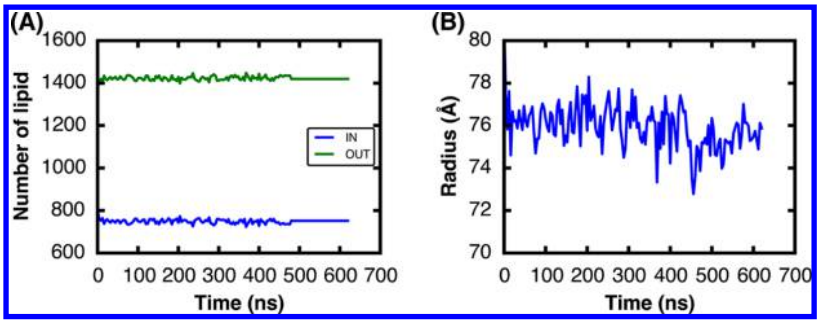


**Figure 8.** Dry POPC vesicle. (A) Number of lipids in the inner and outer layers of the Dry Martini POPC vesicle. (B) Radius of the Dry Martini POPC vesicle.

distributed systems with different sizes. The system size is limited by the maximal number of atoms that CHARMM can handle and also by the server hardware. In the current version, the limit is one million atoms, but it could be increased upon user's request. We note that large Martini systems can also be built using script-base tools such as *insane*,[12] *AlChemBed*,[10] *InflateGRO2*,[8] and *LipidWrapper*,[9] which are advantageous in high-throughput modeling. Compared to these tools, *Martini Maker* is featured in providing an intuitive interface and a set of files that are ready-to-go with the GROMACS simulation package. Our tests demonstrate that the systems generated using *Martini Maker* behave consistently with systems built using *insane*[12] and in other studies.

In the current implementation, electrostatic interactions are calculated with a shift method. However, for the systems where electrostatic interactions are important,[53] it is desirable to use the particle mesh Ewald method[54] in combination with the polarizable water model.[29] This feature will be added in future development. In addition, other future developments include supporting for new lipid types and other classes of biological molecules such as carbohydrates[55] and nucleic acids[56] and building new lipid morphologies such as the hexagonal[57] and cubic[58,59] phases. We expect that *Martini Maker* will be a useful tool for modeling various large, complicated biomolecular systems in a user-friendly way.

## ■ ASSOCIATED CONTENT

### Supporting Information

The Supporting Information is available free of charge on the ACS Publications website at DOI: 10.1021/acs.jctc.5b00513.

Average area per lipid relaxation (Figure S1); number of SDS molecules in contact with the GpA dimer (Figure S2); fitting of $N_{lipid}$ and *Ratio* for DPPC vesicles (Figure S3); linear fitting of area per lipid and parameter *c* and *p* for 17 lipids in Table S3 (Figure S4); lipid types available in *Martini Maker* (Table S1); lipid fatty acid nomenclature (Table S2); fitting results of lipid number and ratio as a function of vesicle radius (Table S3); time required to build different sizes of systems using *Martini Maker* (Table S4) (PDF).

## ■ AUTHOR INFORMATION

### Corresponding Author

*Tel: +1-785-1993; Fax: +1-785-864-5558; E-mail: wonpil@ku.edu.

### Funding

This work was supported in part by NSF ABI-1145987, NIH U54GM087519, and XSEDE TG-MCB070009 (to W.I.). S.J.M. acknowledges funding from The Netherlands Organisation for Scientific Research (NWO) through a TOP-grant.

### Notes

The authors declare no competing financial interest.

## ■ REFERENCES

(1) Lee, E. H.; Hsin, J.; Sotomayor, M.; Comellas, G.; Schulten, K. Discovery through the computational microscope. *Structure* **2009**, *17*, 1295−1306.

(2) Khalili-Araghi, F.; Gumbart, J.; Wen, P. C.; Sotomayor, M.; Tajkhorshid, E.; Schulten, K. Molecular dynamics simulations of membrane channels and transporters. *Curr. Opin. Struct. Biol.* **2009**, *19*, 128−137.

(3) Stansfeld, P. J.; Sansom, M. S. Molecular simulation approaches to membrane proteins. *Structure* **2011**, *19*, 1562−1572.

(4) Ingolfsson, H. I.; Lopez, C. A.; Uusitalo, J. J.; de Jong, D. H.; Gopal, S. M.; Periole, X.; Marrink, S. J. The power of coarse graining in biomolecular simulations. *Wiley Interdiscip. Rev. Comput. Mol. Sci.* **2014**, *4*, 225−248.

(5) Saunders, M. G.; Voth, G. A. Coarse-graining methods for computational biology. *Annu. Rev. Biophys.* **2013**, *42*, 73−93.

(6) Noid, W. G. Perspective: Coarse-grained models for biomolecular systems. *J. Chem. Phys.* **2013**, *139*, 090901.

(7) Marrink, S. J.; Tieleman, D. P. Perspective on the Martini model. *Chem. Soc. Rev.* **2013**, *42*, 6801−6822.

(8) Schmidt, T. H.; Kandt, C. LAMBADA and InflateGRO2: efficient membrane alignment and insertion of membrane proteins for molecular dynamics simulations. *J. Chem. Inf. Model.* **2012**, *52*, 2657−2669.

(9) Durrant, J. D.; Amaro, R. E. LipidWrapper: an algorithm for generating large-scale membrane models of arbitrary geometry. *PLoS Comput. Biol.* **2014**, *10*, e1003720.

(10) Jefferys, E.; Sands, Z. A.; Shi, J.; Sansom, M. S.; Fowler, P. W. Alchembed: A Computational Method for Incorporating Multiple Proteins into Complex Lipid Geometries. *J. Chem. Theory Comput.* **2015**, *11*, 2743−2754.

(11) Stansfeld, P. J.; Goose, J. E.; Caffrey, M.; Carpenter, E. P.; Parker, J. L.; Newstead, S.; Sansom, M. S. MemProtMD: Automated Insertion of Membrane Protein Structures into Explicit Lipid Membranes. *Structure* **2015**, *23*, 1350−1361.

(12) Wassenaar, T. A.; Ingólfsson, H. I.; Böckmann, R. A.; Tieleman, D. P.; Marrink, S. J. Computational Lipidomics with insane: A Versatile Tool for Generating Custom Membranes for Molecular Simulations. *J. Chem. Theory Comput.* **2015**, *11*, 2144−2155.

(13) Wassenaar, T. A.; Pluhackova, K.; Moussatova, A.; Sengupta, D.; Marrink, S. J.; Tieleman, D. P.; Böckmann, R. A. High-Throughput Simulations of Dimer and Trimer Assembly of Membrane Proteins. The DAFT Approach. *J. Chem. Theory Comput.* **2015**, *11*, 2278−2291.

(14) Jo, S.; Kim, T.; Iyer, V. G.; Im, W. CHARMM-GUI: a web-based graphical user interface for CHARMM. *J. Comput. Chem.* **2008**, *29*, 1859−1865.

(15) Brooks, B. R.; Brooks, C. L., 3rd; Mackerell, A. D., Jr.; Nilsson, L.; Petrella, R. J.; Roux, B.; Won, Y.; Archontis, G.; Bartels, C.;



DOI: 10.1021/acs.jctc.5b00513
*J. Chem. Theory Comput.* 2015, 11, 4486−4494

Boresch, S.; Caflisch, A.; Caves, L.; Cui, Q.; Dinner, A. R.; Feig, M.; Fischer, S.; Gao, J.; Hodoscek, M.; Im, W.; Kuczera, K.; Lazaridis, T.; Ma, J.; Ovchinnikov, V.; Paci, E.; Pastor, R. W.; Post, C. B.; Pu, J. Z.; Schaefer, M.; Tidor, B.; Venable, R. M.; Woodcock, H. L.; Wu, X.; Yang, W.; York, D. M.; Karplus, M. CHARMM: the biomolecular simulation program. *J. Comput. Chem.* **2009**, *30*, 1545−1614.

(16) Phillips, J. C.; Braun, R.; Wang, W.; Gumbart, J.; Tajkhorshid, E.; Villa, E.; Chipot, C.; Skeel, R. D.; Kale, L.; Schulten, K. Scalable molecular dynamics with NAMD. *J. Comput. Chem.* **2005**, *26*, 1781−1802.

(17) Pronk, S.; Pall, S.; Schulz, R.; Larsson, P.; Bjelkmar, P.; Apostolov, R.; Shirts, M. R.; Smith, J. C.; Kasson, P. M.; van der Spoel, D.; Hess, B.; Lindahl, E. GROMACS 4.5: a high-throughput and highly parallel open source molecular simulation toolkit. *Bioinformatics* **2013**, *29*, 845−854.

(18) Case, D. A.; Cheatham, T. E., 3rd; Darden, T.; Gohlke, H.; Luo, R.; Merz, K. M., Jr.; Onufriev, A.; Simmerling, C.; Wang, B.; Woods, R. J. The Amber biomolecular simulation programs. *J. Comput. Chem.* **2005**, *26*, 1668−1688.

(19) Eastman, P.; Friedrichs, M. S.; Chodera, J. D.; Radmer, R. J.; Bruns, C. M.; Ku, J. P.; Beauchamp, K. A.; Lane, T. J.; Wang, L. P.; Shukla, D.; Tye, T.; Houston, M.; Stich, T.; Klein, C.; Shirts, M. R.; Pande, V. S. OpenMM 4: A Reusable, Extensible, Hardware Independent Library for High Performance Molecular Simulation. *J. Chem. Theory Comput.* **2013**, *9*, 461−469.

(20) Wu, E. L.; Cheng, X.; Jo, S.; Rui, H.; Song, K. C.; Davila-Contreras, E. M.; Qi, Y.; Lee, J.; Monje-Galvan, V.; Venable, R. M.; Klauda, J. B.; Im, W. CHARMM-GUI Membrane Builder toward realistic biological membrane simulations. *J. Comput. Chem.* **2014**, *35*, 1997−2004.

(21) Jo, S.; Lim, J. B.; Klauda, J. B.; Im, W. CHARMM-GUI Membrane Builder for mixed bilayers and its application to yeast membranes. *Biophys. J.* **2009**, *97*, 50−58.

(22) Jo, S.; Kim, T.; Im, W. Automated builder and database of protein/membrane complexes for molecular dynamics simulations. *PLoS One* **2007**, *2*, e880.

(23) Cheng, X.; Jo, S.; Lee, H. S.; Klauda, J. B.; Im, W. CHARMM-GUI micelle builder for pure/mixed micelle and protein/micelle complex systems. *J. Chem. Inf. Model.* **2013**, *53*, 2171−2180.

(24) Qi, Y.; Cheng, X.; Han, W.; Jo, S.; Schulten, K.; Im, W. CHARMM-GUI PACE CG Builder for solution, micelle, and bilayer coarse-grained simulations. *J. Chem. Inf. Model.* **2014**, *54*, 1003−1009.

(25) Marrink, S. J.; de Vries, A. H.; Mark, A. E. Coarse Grained Model for Semiquantitative Lipid Simulations. *J. Phys. Chem. B* **2004**, *108*, 750−760.

(26) Monticelli, L.; Kandasamy, S. K.; Periole, X.; Larson, R. G.; Tieleman, D. P.; Marrink, S.-J. The MARTINI Coarse-Grained Force Field: Extension to Proteins. *J. Chem. Theory Comput.* **2008**, *4*, 819−834.

(27) Marrink, S. J.; Risselada, H. J.; Yefimov, S.; Tieleman, D. P.; de Vries, A. H. The MARTINI force field: coarse grained model for biomolecular simulations. *J. Phys. Chem. B* **2007**, *111*, 7812−7824.

(28) de Jong, D. H.; Singh, G.; Bennett, W. F. D.; Arnarez, C.; Wassenaar, T. A.; Schafer, L. V.; Periole, X.; Tieleman, D. P.; Marrink, S. J. Improved Parameters for the Martini Coarse-Grained Protein Force Field. *J. Chem. Theory Comput.* **2013**, *9*, 687−697.

(29) Yesylevskyy, S. O.; Schafer, L. V.; Sengupta, D.; Marrink, S. J. Polarizable water model for the coarse-grained MARTINI force field. *PLoS Comput. Biol.* **2010**, *6*, e1000810.

(30) Arnarez, C.; Uusitalo, J. J.; Masman, M. F.; Ingolfsson, H. I.; de Jong, D. H.; Melo, M. N.; Periole, X.; de Vries, A. H.; Marrink, S. J. Dry Martini, a Coarse-Grained Force Field for Lipid Membrane Simblations with Implicit Solvent. *J. Chem. Theory Comput.* **2015**, *11*, 260−275.

(31) Periole, X.; Cavalli, M.; Marrink, S. J.; Ceruso, M. A. Combining an Elastic Network With a Coarse-Grained Molecular Force Field: Structure, Dynamics, and Intermolecular Recognition. *J. Chem. Theory Comput.* **2009**, *5*, 2531−2543.

(32) Ingolfsson, H. I.; Melo, M. N.; van Eerden, F. J.; Arnarez, C.; Lopez, C. A.; Wassenaar, T. A.; Periole, X.; de Vries, A. H.; Tieleman, D. P.; Marrink, S. J. Lipid organization of the plasma membrane. *J. Am. Chem. Soc.* **2014**, *136*, 14554−14559.

(33) Jo, S.; Cheng, X.; Islam, S. M.; Huang, L.; Rui, H.; Zhu, A.; Lee, H. S.; Qi, Y.; Han, W.; Vanommeslaeghe, K.; MacKerell, A. D., Jr.; Roux, B.; Im, W. CHARMM-GUI PDB manipulator for advanced modeling and simulations of proteins containing nonstandard residues. *Adv. Protein Chem. Struct. Biol.* **2014**, *96*, 235−265.

(34) Berman, H. M.; Westbrook, J.; Feng, Z.; Gilliland, G.; Bhat, T. N.; Weissig, H.; Shindyalov, I. N.; Bourne, P. E. The Protein Data Bank. *Nucleic Acids Res.* **2000**, *28*, 235−242.

(35) Lomize, M. A.; Lomize, A. L.; Pogozheva, I. D.; Mosberg, H. I. OPM: orientations of proteins in membranes database. *Bioinformatics* **2006**, *22*, 623−625.

(36) Kabsch, W.; Sander, C. Dictionary of protein secondary structure: Pattern recognition of hydrogen-bonded and geometrical features. *Biopolymers* **1983**, *22*, 2577−2637.

(37) Risselada, H. J.; Mark, A. E.; Marrink, S. J. Application of mean field boundary potentials in simulations of lipid vesicles. *J. Phys. Chem. B* **2008**, *112*, 7438−7447.

(38) Risselada, H. J.; Marrink, S. J. Curvature effects on lipid packing and dynamics in liposomes revealed by coarse grained molecular dynamics simulations. *Phys. Chem. Chem. Phys.* **2009**, *11*, 2056−2067.

(39) Berendsen, H. J. C.; Postma, J. P. M.; Vangunsteren, W. F.; Dinola, A.; Haak, J. R. Molecular-Dynamics with Coupling to an External Bath. *J. Chem. Phys.* **1984**, *81*, 3684−3690.

(40) Bussi, G.; Donadio, D.; Parrinello, M. Canonical sampling through velocity rescaling. *J. Chem. Phys.* **2007**, *126*, 014101.

(41) Van Gunsteren, W. F.; Berendsen, H. J. C. A Leap-Frog Algorithm for Stochastic Dynamics. *Mol. Simul.* **1988**, *1*, 173−185.

(42) Humphrey, W.; Dalke, A.; Schulten, K. VMD: Visual molecular dynamics. *J. Mol. Graphics* **1996**, *14*, 33−38.

(43) Sukharev, S. I.; Blount, P.; Martinac, B.; Blattner, F. R.; Kung, C. A large-conductance mechanosensitive channel in E. coli encoded by mscL alone. *Nature* **1994**, *368*, 265−268.

(44) Louhivuori, M.; Risselada, H. J.; van der Giessen, E.; Marrink, S. J. Release of content through mechano-sensitive gates in pressurized liposomes. *Proc. Natl. Acad. Sci. U. S. A.* **2010**, *107*, 19856−19860.

(45) Steinbacher, S.; Bass, R.; Strop, P.; Rees, D. C.; Owen, P. H. Structures of the Prokaryotic Mechanosensitive Channels MscL and MscS. *Curr. Top. Membr.* **2007**, *58*, 1−24.

(46) Jalili, S.; Akhavan, M. A coarse-grained molecular dynamics simulation of a sodium dodecyl sulfate micelle in aqueous solution. *Colloids Surf., A* **2009**, *352*, 99−102.

(47) Gao, J.; Ge, W.; Hu, G. H.; Li, J. H. From homogeneous dispersion to micelles - A molecular dynamics simulation on the compromise of the hydrophilic and hydrophobic effects of sodium dodecyl sulfate in aqueous solution. *Langmuir* **2005**, *21*, 5223−5229.

(48) Marrink, S. J.; Mark, A. E. Molecular dynamics simulation of the formation, structure, and dynamics of small phospholipid vesicles. *J. Am. Chem. Soc.* **2003**, *125*, 15233−15242.

(49) Shinoda, W.; DeVane, R.; Klein, M. L. Zwitterionic Lipid Assemblies: Molecular Dynamics Studies of Monolayers, Bilayers, and Vesicles Using a New Coarse Grain Force Field. *J. Phys. Chem. B* **2010**, *114*, 6836−6849.

(50) Shillcock, J. C. Spontaneous vesicle self-assembly: a mesoscopic view of membrane dynamics. *Langmuir* **2012**, *28*, 541−547.

(51) MacKenzie, K. R.; Prestegard, J. H.; Engelman, D. M. A transmembrane helix dimer: structure and implications. *Science* **1997**, *276*, 131−133.

(52) Braun, R.; Engelman, D. M.; Schulten, K. Molecular Dynamics Simulations of Micelle Formation around Dimeric Glycophorin A Transmembrane Helices. *Biophys. J.* **2004**, *87*, 754−763.

(53) Rzepiela, A. J.; Sengupta, D.; Goga, N.; Marrink, S. J. Membrane poration by antimicrobial peptides combining atomistic and coarse-grained descriptions. *Faraday Discuss.* **2010**, *144*, 431−443.



DOI: 10.1021/acs.jctc.5b00513
*J. Chem. Theory Comput.* 2015, 11, 4486−4494

(54) Essmann, U.; Perera, L.; Berkowitz, M. L.; Darden, T.; Lee, H.; Pedersen, L. G. A Smooth Particle Mesh Ewald Method. *J. Chem. Phys.* **1995**, *103*, 8577−8593.
(55) López, C. A.; Rzepiela, A. J.; de Vries, A. H.; Dijkhuizen, L.; Hünenberger, P. H.; Marrink, S. J. Martini Coarse-Grained Force Field: Extension to Carbohydrates. *J. Chem. Theory Comput.* **2009**, *5*, 3195−3210.
(56) Uusitalo, J. J.; Ingólfsson, H. I.; Akhshi, P.; Tieleman, D. P.; Marrink, S. J. Martini Coarse-Grained Force Field: Extension to DNA. *J. Chem. Theory Comput.* **2015**, *11*, 3932.
(57) Sodt, A. J.; Pastor, R. W. Bending free energy from simulation: correspondence of planar and inverse hexagonal lipid phases. *Biophys. J.* **2013**, *104*, 2202−2211.
(58) Fuhrmans, M.; Knecht, V.; Marrink, S. J. A single bicontinuous cubic phase induced by fusion peptides. *J. Am. Chem. Soc.* **2009**, *131*, 9166−9167.
(59) Khelashvili, G.; Albornoz, P. B.; Johner, N.; Mondal, S.; Caffrey, M.; Weinstein, H. Why GPCRs behave differently in cubic and lamellar lipidic mesophases. *J. Am. Chem. Soc.* **2012**, *134*, 15858−15868.


DOI: 10.1021/acs.jctc.5b00513
*J. Chem. Theory Comput.* 2015, 11, 4486−4494